

FLUID FLOW AND HEAT TRANSFER IN MICROCHANNEL DEVICES FOR COOLING APPLICATIONS: EXPERIMENTAL AND NUMERICAL APPROACHES

Pontes P, Martins L., Gonçalves I, Manetti L, Andreaki, M, Georgoulas, G., Moreira A.L.N. and Moita A.S.*
Author for correspondence

CINAMIL – Military Academy Research Center, Department of Exact Sciences and Engineering, Portuguese Military Academy, R. Gomes Freire 203, 1169-203 Lisbon, Portugal

IN+ Center for Innovation, Technology and Policy Research, Instituto Superior Técnico, Universidade de Lisboa. Av. Rovisco Pais, 1049-001 Lisboa, Portugal

UNESP –São Paulo State University, School of Engineering, Post-Graduation Program in Mechanical Engineering, Av. Brasil, 56, 15385-000, Ilha Solteira, SP, Brazil

IFMS - Federal Institute of Education, Science and Technology of Mato Grosso do Sul, Campus Campo Grande, Campo Grande, MS, Brazil

Advanced Engineering Centre, School of Computing Engineering and Mathematics, Cockcroft Building, University of Brighton, Lewes Road, Brighton, BN2 4GJ, United Kingdom

E-mail: anamoita@tecnico.ulisboa.pt moita.asoh@exercito.pt

ABSTRACT

Microchannel heat sinks are pointed to have a great potential in cooling systems. This paper presents a systematic study to develop a microchannel heat sink to be used in PV panels cooling. A systematic experimental approach is used to optimize the heat sink geometry. Then the potential advantage of using flow boiling conditions is explored in both numerical and experimental approaches. The results show that a heat exchanger with thin walls and wide channels can dissipate a greater amount of heat. Comparing the results obtained for one and two-phase flow conditions, one must conclude that although in the boiling tests the heat transfer coefficient was higher, the cooling method with single-phase flow using water dissipated a greater amount of heat, which was mainly due to flow instabilities. In this context, the numerical work clearly evidences that boiling can be an advantage in microchannel heat sinks, as long as the flow is controlled. The work also shows that the considered numerical simulation tool is sensitive enough to quantify the heat transfer enhancement due to boiling within the examined microchannel paths.

INTRODUCTION

Over the years, several studies have been carried out to design effective cooling systems for solar panels with a high concentration of solar radiation. Passive cooling methods are reliable, do not consume system energy, and are cheaper, however, for a heat exchanger to perform better at this high solar radiation, it will be necessary to implement an active cooling system.

Active cooling with microchannels and using water as a coolant has a low thermal resistance, allowing greater heat dissipation and consequently better cooling [1].

The geometrical parameters of a heat exchanger influence the thermal performance in the cooling. Raghuraman *et al.* [2] performed a numerical and experimental work where they studied the influence of the aspect ratio on thermal performance using a heat exchanger with rectangular channels. The three heat

exchangers tested have an aspect ratio of 20, 30, and 46.6. Through experimental and numerical tests, the results obtained included the parameters of pressure drop, friction factor, Nusselt number, thermal resistance, pumping power, and Poiseuille number, Raghuraman *et al.* [2] concluded that it is preferable to implement the exchanger with intermediate dimensions since it was responsible for removing a greater amount of heat, while keeping the other parameters at a level that is feasible for the project. Upadhye and Kandlikar [3] carried out numerical work to evaluate the effect of the heat exchanger geometry to cool an electronic chip with dimensions of 25mm by 25mm. For an imposed flow of 100 /cm², they concluded that a channel with smaller dimensions depicts a better cooling performance.

Wang *et al.* [4] tested microchannels with a rectangular, trapezoidal, and triangular section, concluding that channels with a higher aspect ratio and smaller hydraulic diameter have a lower thermal resistance but a greater pressure drop. Wang *et al.* [4] also concluded that with the increase in the number of channels, the thermal resistance decreases, but in return, there will be an increase in the pressure drop in the exchanger. Xie *et al.* [5] tested an exchanger with mini-channels to cool an area of 20 mm x 20 mm, concluding that narrower channels have a better performance, balancing heat transfer and pressure drop, when compared to wider channels.

All the aforementioned studies were performed with single-phase fluid flows. By allowing the refrigerant to boil, the latent heat of the fluid is used to increase the heat flux removed. Despite presenting this added value, multiphase flow is more difficult to model, predict and control. Hetsroni *et al.* [6] conducted an experimental investigation on the effect of boiling on the cooling of electronic devices, using Vertrel XF as a boiling refrigerant, and finally compared it with the results obtained using water. The temperature gradient using boiling did not exceed 5K, while in water cooling the temperature difference was 20 K. However, the growth and consequent collapse of the vapor bubbles caused fluctuations in the pressure drop and decreased the heat transfer coefficient. In the work carried out by

Tran *et al.* [7] it was concluded that in smaller channels, the nucleation mechanism is dominant compared to the convection mechanism, thus concluding that boiling in microchannels increases heat transfer.

The brief literature review performed here shows a wide range of studies on flow boiling heat transfer in microchannels. However, geometry optimization (balancing heat transfer and pressure drops) is mostly taken by a trial-and-error approach and the potential advantages of actually using boiling to enhance the heat transfer are not clearly presented, as they are presented against a large number of obstacles. In line with this, the present work addresses a systematic approach where the geometry is firstly optimized in a single-phase study. Then, the optimized geometry is tested under two-phase flow conditions, which are then discussed in detail in a numerical approach.

NOMENCLATURE

H	[mm]	Height of the computational domain
L	[mm]	Length of the computational domain
L^*	[mm]	Dimensionless length of the computational domain
W	[]	Width of the computational domain
Special characters		
θ	[°]	Contact angle
Subscripts		
e		Equilibrium
l		Liquid
s		Solid

EXPERIMENTAL METHOD

Experimental setup

Figure 1 shows, schematically, the components used in the experimental setup and how they are interconnected. The syringe pump injects the fluid that enters the microchannel system (5). The fluid comes out preheated from the syringe, through a heating system composed of a sleeve of electrical resistances, thus maintaining the fluid at the desired temperature and always constant. To control the conditions of the experiment, a type K thermocouple was placed at the entrance of the microchannel heat sink, and this temperature information was sent to a DT9828 acquisition system (4). Water and HFE7100, from 3M were used as the working fluids.

The microchannels heat sinks, made from PDMS – Polydimethylsiloxane, are glued on a 20 μm stainless-steel foil (AISI 304) (6) which is heated by the Joule effect using a direct current power source (8) - Model HP 6274B A.D. The electric current is supplied to the steel foil through electrical cables welded at the ends of the foil (9). The heated steel foil simulates the heating phenomenon that occurs with photovoltaic cells subjected to solar radiation. The cooling of the steel foil caused by the passage of the fluid is captured by the high-speed thermographic Onca MWIR-InSb-320 (12), which is placed in a lower plane than the microchannel system, thus allowing to capture temperature variations on the stainless-steel foil. The

back side of the foil is black painted (the paint has an emissivity of 0.96). Calibration and post-processing procedures were performed as in Pontes *et al.* [8]. To be able to observe the behaviour of the fluid during the flow, a high-speed camera - Phantom v4.2 Vision Research (7) was placed perpendicularly to the upper face of the microchannels heat sink, allowing the registration of the different regimes of flow observed during the phase change of the fluid, and their effect on the flow dynamics. After passing through the channels causing the steel foil to cool, the fluid exits at the other end of the system (11) and is sent to a reservoir (10). To validate the effect of the geometries in terms of pressure drop, absolute pressure sensors - Wika A-10 - were placed at the entrance and exit of the microchannels heat sink, thus allowing to obtain the value of the pressure drop and then evaluate the consequent friction factor of each of the geometry. The pressure values are sent to an NI USB-6008 data reader (2). The pressure and temperature values collected by the two acquisition systems and the images obtained by the two cameras are sent to the computer (3) for future treatment of the data in a LABVIEW routine previously developed for this purpose.

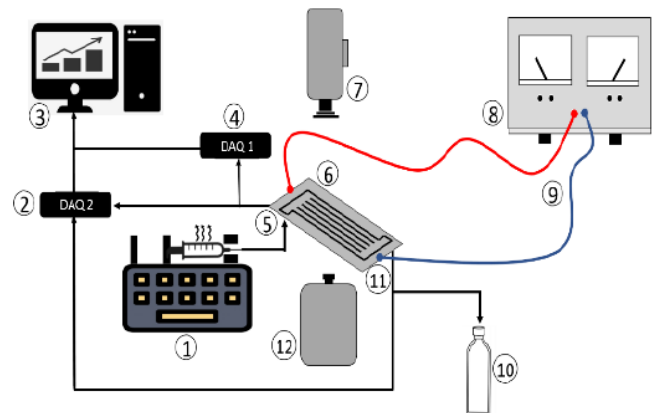


Figure 1 Schematic of the experimental setup: (1) Syringe pump with a heater, (2) DAQ1, (3) PC, (4) DAQ2, (5) heat sink inlet, (6) steel foil, (7) high-speed camera, (8) DC power supply, (9) electric cables, (10) reservoir, (11) heat sink outlet, (12) infrared thermography.

Fabrication and characterization of the microchannel heat sink

The various geometries of microchannel heat exchangers used in this work were prepared with 3D printing molds in PDMS. Three different dimensions of the wall and channel width were used: 250 μm , 500 μm and 750 μm , thus resulting in a combination of nine testing geometries. The height was kept constant in all heat sinks, equal to 1 mm. The geometry is limited to a fixed area of 2cm² which is the cooling area of interest for our study. Therefore, geometries with wider channels and walls have a smaller number of fluid passage channels. This number increases when narrowing the dimensions of the heat sink.

Characterization of the surfaces

The steel foil and the PDMS heat sink surfaces were characterized in terms of wettability (quantified by the

equilibrium contact angle), as in the microscale, it is a parameter with significant relevance.

The obtained values show that the steel foil presents a hydrophilic behaviour ($\theta_e < 90^\circ$) while the PDMS has a hydrophobic behaviour ($90^\circ < \theta_e < 150^\circ$). HFE 7100 has very high wettability at all tested surfaces, depicting a contact angle close to zero, both for the steel foil and for the PDMS.

Experimental procedure

In the first phase and to study the effect of the microchannel geometry, tests were performed for the five flowrates that were considered here, namely: 5 ml/min; 7 ml/min; 10 ml/min; 15 ml/min; 20 ml/min, always using water at room temperature. After getting the best geometry, HFE 7100 was used to test the effect of boiling on cooling. For that, three geometries were used and all the steps above were repeated for the same volumetric flow values, testing and observing the cooling potential of a heated surface through boiling. For statistical purposes, each test was repeated five times. The high-speed camera Phantom V4.2 was only used in the tests in which the HFE 7100 boiled, allowing to observe the different flow regimes and some flow phenomena due to the change of phase of the fluid. High-speed videos were recorded at 1000 frames/s, with a resolution of 512px x 512px and thermographic videos were recorded at 60frames/s with a resolution of 320px x 256 px.

NUMERICAL METHOD

A preliminary 3D transient numerical investigation has also been performed focusing in one single channel path, with a particular width and height and two particular flow rates among the flow boiling cases of HFE7100 that were tested experimentally. The main aim is to explore the generated bubble dynamics in relation to the heat transfer characteristics for the first transient stage of the two-phase flow development considering the first 10 ms after a single nucleation event. The simulations were performed by utilising a custom, enhanced VOF-based solver that has been developed in OpenFOAM CFD Toolbox. Due to the high computational cost a channel length L of only 4.80 mm was considered for all cases. The working fluid was HFE7100, while the applied heat flux was 1386.83 W/m^2 and the flow rates were 5 ml/min and 10 ml/min, respectively. The utilised numerical solver has been expensively validated and applied in the past against adiabatic and diabatic droplet and bubble dynamics and particularly for flow boiling applications. Enhancements of the proposed solver with respect to the original VOF solver of OpenFOAM that are necessary for the purposes of the present numerical investigation include a treatment for spurious currents dampening (a well-known defect of VOF methods), an improved accurate dynamic contact angle treatment to account for wettability effects, a phase-change model as well as conjugate heat transfer between solid and fluid domains. Further details regarding the proposed implementations as well as validation and application cases can be found in [9-11]. The computational mesh has been generated by discretising the computational domain in two parts: the solid domain and the fluid domain. A uniform, structured computational mesh, consisting of uniform hexahedral elements was utilised. The physical dimensions of the fluid domain

(length, height and width) are $L=4.80 \text{ mm}$, $H = 1.00 \text{ mm}$, $W = 0.50 \text{ mm}$ and the solid domain dimensions are $L_s = 4.80 \text{ mm}$, $H_s = 0.02 \text{ mm}$, $W_s = 0.50 \text{ mm}$, respectively. The generated computational geometry, the mesh and the applied boundary conditions are illustrated in Figure 2. The total number of cells sums up to 20352000, considering both fluid and solid domains.

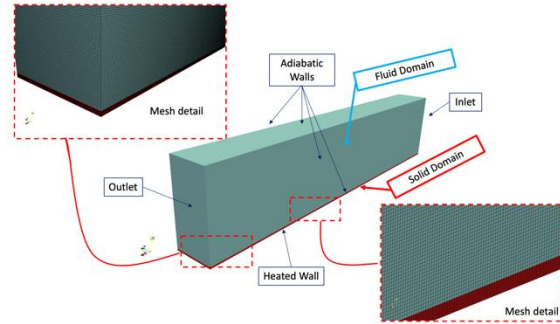


Figure 2 Computational domain, mesh and boundary conditions used for the numerical simulations.

In order to simulate as realistic as possible the case of HFE7100 flow boiling within a microchannel path, a conjugate heat transfer model was utilised. The numerical simulations were performed in two main stages. At the first stage, within the microchannel, a liquid is flowing at saturation temperature and with constant uniform velocity from the inlet, whereas in the solid domain, a constant heat flux is applied at its bottom boundary. This stage is run up for 0.5 seconds of real flow until the initial thermal and hydrodynamic boundary layers are fully developed. At the second stage, 30 arbitrary located bubble seeds are positioned on the conjugate boundary, representing multiple simultaneous nucleation sites. As mentioned previously, due to the high computational cost, a single nucleation event is simulated (without additional bubble nucleation) and the simulations for both considered flow rates are focused on the first 10 ms after the simultaneous nucleation sites activation. The initial condition for the second and main stage of the simulations is illustrated indicatively for the low flow rate case in Figure 3.

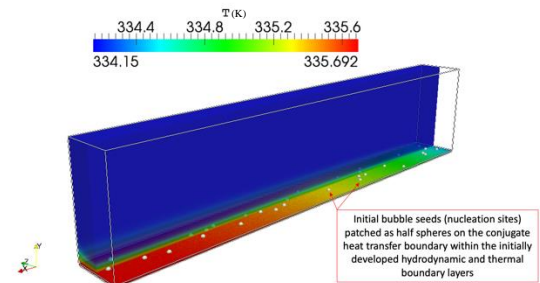


Figure 3 Initial condition for two-phase flow stage of numerical simulations.

At this point it should be mentioned that the number of nucleation sites is arbitrary selected, and, in the future, it should be estimated according to experimental observations, as the utilise numerical model does not account for nucleation and the nucleation is initiated artificially in order to initiate the bubble growth and detachment process. Unfortunately, for the particular

selected cases due to low quality of high-speed images this information could not be extracted. However, despite this fact, the purpose of these preliminary numerical simulations is to illustrate that detailed transient quantitative information can be extracted, revealing information that cannot be quantified experimentally.

RESULTS AND DISCUSSION

Effect of heat sink geometry on cooling

Figure 4 shows the values of pressure drop and pumping power, for heat sink geometries with the same microchannels wall width and with the channels width varying between 250 μm and 750 μm . Analyzing the data in the figure there is an increasing linear trend of pressure drop with increasing flow rate. It can also be seen that with the widening of the channel, the pressure drops in the exchanger are smaller. The pumping power is augmented with the increase in the flow of fluid drained. The pumping power also increases in the narrower channels. Figure 5 shows the values of the heat transfer coefficient and the dissipated heat flux when cooling the steel foil, as a function of the flow Reynolds number. An increasing linear trend for the heat transfer coefficient is observed with the Reynolds number. The heat transfer coefficient also increases with the widening of the channel. As for the values of the dissipated heat flux due to cooling, the results suggest that with the increase in the flowrate, more heat is removed from the heated surface and its value is greater, the wider the channel. For lower Reynolds number values, a higher heat transfer coefficient is observed when the channel is wider. Figure 6 depicts the values of pressure drop and pumping power, for geometries with the same channel width and with the wall width varying between 250 μm and 750 μm . Analyzing the data in the figure there is an increasing linear trend for pressure drop, with increasing flowrate. It can also be seen that with the widening of the wall, the pressure drops in the exchanger are greater. The pumping power is greater with the increase in the flow of fluid drained, and an increase is registered in the wider walls. Figure 7 shows the values of the heat transfer coefficient and the dissipated heat flux when cooling the steel foil. An increasing linear trend for the heat transfer coefficient is observed with the Reynolds number and its value also increases with the narrowing of the wall. As for the values of the dissipated heat flux due to cooling, it appears that with the increase in the flowrate, more heat is removed from the heated surface and its value is greater, the narrower the wall. For lower Reynolds number values, a higher heat transfer coefficient is observed when the wall is narrower.

After evaluated the effect of the geometry on cooling, it is concluded that an exchanger with thin walls and wide channels leads to better performance in cooling the heated surface and has lower pressure drops in its operation. A geometry with thinner walls has a greater number of channels, so there is more space to exchange heat. The results obtained for the effect of the channel width are inconsistent with the literature [3-5]. A possible justification for the results obtained in this experimental work is the difference in the properties of the base and the exchanger. Since the base is a steel foil and the heat exchanger is made of

PDMS, there will be more heat exchanges with the base than with the heat sink.

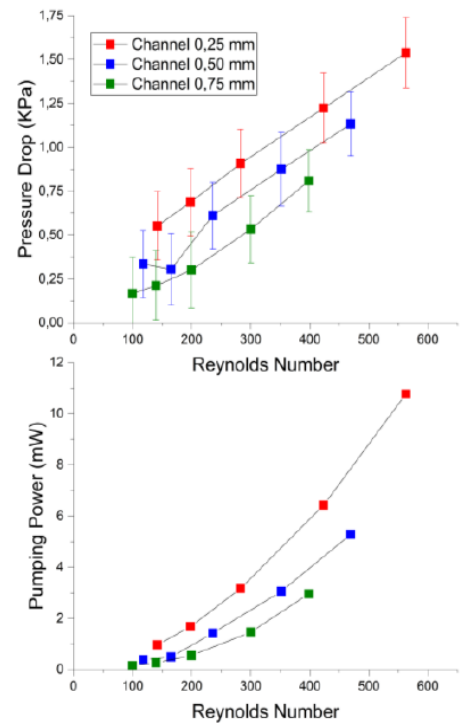


Figure 4 Pressure drop and pumping power for single phase water flow in the heat sinks with varying channel width.

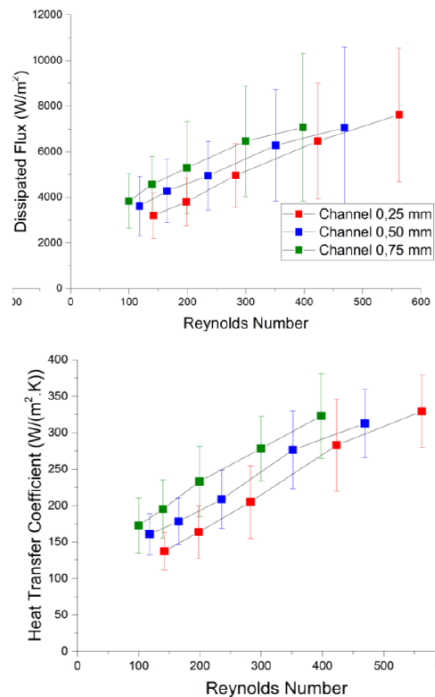


Figure 5 Dissipated heat flux and heat transfer coefficient for single phase water flow in the heat sinks with varying channel width.

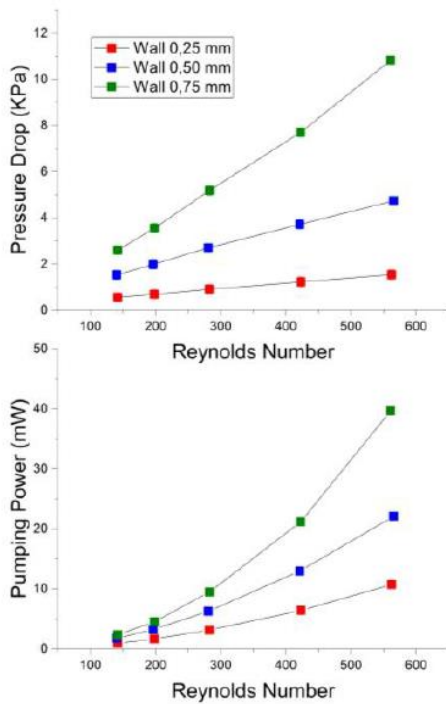


Figure 6 Pressure drop and pumping power for single phase water flow in the heat sinks with varying wall width.

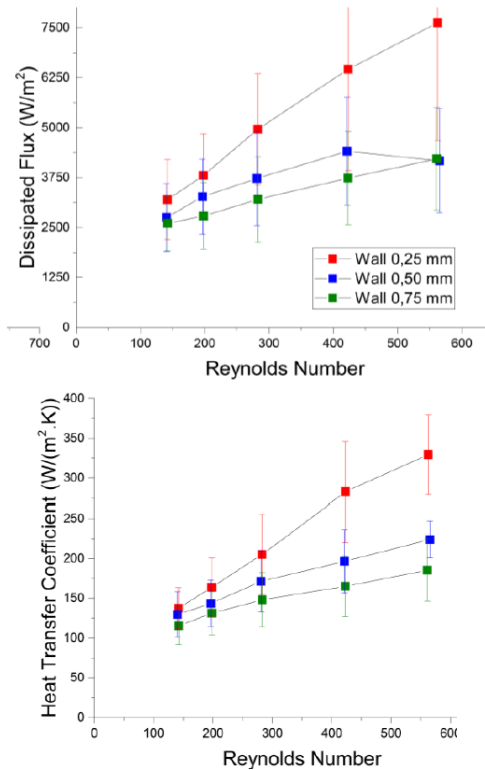


Figure 7 Dissipated heat flux and heat transfer coefficient for single phase water flow in the heat sinks with varying wall width.

Potential of using flow boiling heat transfer

The results obtained with phase change, which are not shown here due to paper length constraints were strongly affected by flow instability, which leads to large values fluctuation. To better understand these fluctuations, a detailed high-speed thermal analysis was performed together with a thermographic analysis. Although the method of cooling through the latent heat of vaporizing a fluid has great potential to dissipate large amounts of heat, it is a method that requires a more substantial control of the operating conditions of the system. One of the problems that can occur is the trapping of vapor bubbles in the channels, thus making it difficult for the fluid to pass through the exchanger channels. High-speed images, which are not shown here due to paper length constraints clearly show that vapour bubbles enter the channel closest to the hole through which the fluid is injected. As the flow develops, the presence of bubbles can be observed in all the channels of the exchanger. Since all flow rates used in the tests were low, it was only possible to identify the biphasic flow regime with bubbles (bubbly flow). High-speed images also depict a reversal of the flow of steam in some channels. This flow reversal causes pressure, flow rate, and temperature fluctuations. Due to the reversal of the flow in only a few channels, there is a poor distribution of the fluid through the channels, making the cooling less homogeneous on the surface. The presence of these masses of steam in the channels can obstruct the passage of fluid, generating a large pressure drop. This behavior, which cannot be completely described by the experiments is explored in the numerical results presented in the following paragraphs.

Numerical Simulation Results

A qualitative illustration of the numerical simulation predictions for the low flow rate case (5 ml/min) can be seen in Figure 8 indicatively, where a top view and an isometric view of the spatial and temporal evolution of the vapour bubbles, within the considered microchannel path, are depicted. In total, three common successive time instants are shown. As it can be observed, a bubbly flow regime is developed after the considered initial nucleation event which agrees with the prevailing flow regime that was observed in the experimental measurements. Moreover, the expected cooling of the solid domain due to the contact line evaporation at the meniscus of the considered bubble seeds is observed. A similar evolution has also been observed for the higher flow rate considered (10 ml/min).

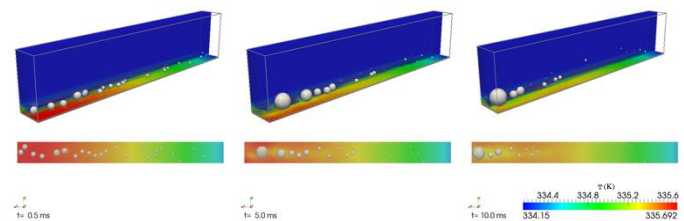


Figure 8 Spatial and temporal evolution of vapour/liquid interface for the 5 ml/min flow rate case (grey surface). The temperature fields in the liquid and solid domain are also illustrated using the supplied colour legend.

However, to quantify the effect of the considered nucleation event on the heat transfer characteristics within the considered

microchannel path time averaged local Nu number is plotted for both flow rates together with the corresponding Nu number at the end of the initial single-phase stage of the simulations (Figure 9).

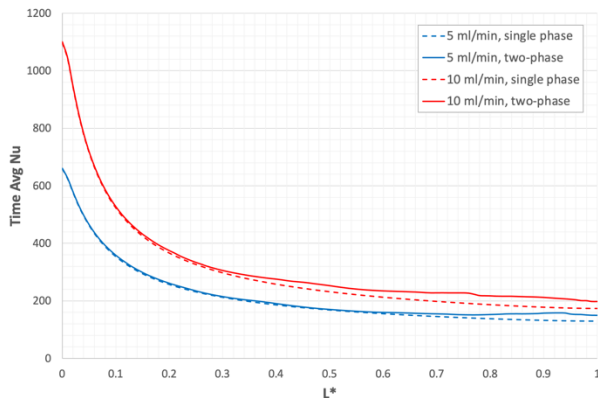


Figure 7 Time averaged local Nu versus dimensionless channel path length L^* .

As it can be observed and as it was expected the heat transfer performance of the higher flow rate is higher. In both cases the considered nucleation event due to the underpinned contact line evaporation and the associated bubble growth and detachment increases the local heat transfer. The percentage increase is low due to the fact that only a single nucleation event is considered. It has been shown in a similar investigation in [11] that considering seven successive multiple nucleation events, it can additionally enhance heat transfer by values of more than 40%. From these preliminary numerical simulation results, it can be concluded that the considered numerical simulation tool is sensitive enough to quantify the heat transfer enhancement due to boiling within the examined microchannel paths. It is quite promising that despite the modelling assumptions the predicted two-phase flow regime agrees with the experimental observations. For the future more realistic initial distribution of nucleation sites and bubble nucleation frequencies that agree with the experimental measurements are going to be considered as well as longer channel paths and even parallel microchannels to examine and quantify the flow reversals observed in the experimental visualizations.

CONCLUSION

In summary, the results obtained in this work indicate that a heat exchanger with thin walls and wide channels can dissipate a greater amount of heat. Comparing the results obtained with single and two-phase flows, it is concluded that, although in the boiling tests the heat transfer coefficient was higher, the cooling method with single-phase flow using water dissipated a greater amount of heat due to issues related to 2 phase flow fluctuations. The pumping power values obtained in the tests performed are higher in geometries where the channels are thinner and the walls wider. Despite being an important parameter in the design of an exchanger, the values obtained in this experiment are low, when compared to the heat dissipated. This confirms the great potential that a microchannel heat sink has in cooling, making its implementation in high concentration solar panels worthwhile,

which was the main motivation for this study. To better understand the potential of flow boiling in heat transfer enhancement, a numerical study was performed. The results clearly evidence that boiling can be an advantage in microchannel heat sinks, as long as the flow is controlled. The work also evidences that the considered numerical simulation tool is sensitive enough to quantify the heat transfer enhancement due to boiling within the examined microchannel paths.

ACKNOWLEDGEMENTS

Authors acknowledge to Fundação para a Ciência e a Tecnologia, FCT, for partially financing this project through projects JICAM/0003/2017 and for funding the scholarship SFRH/BD/149286/2019.

REFERENCES

- [1] Royné, A., Dey, C.J. and Mills, D.R., Cooling of photovoltaic cells under concentrated illumination: a critical review», *Sol. Energy Mater. Sol. Cells*, vol. 86, n. 4, 2005, pp. 451–483.
- [2] Raghuraman, D.R.S., Raj, R.T.K., Nagarajan, P.K. and Rao, B.V.A., Influence of aspect ratio on the thermal performance of rectangular shaped micro channel heat sink using CFD code, *Alex. Eng. J.*, vol. 56, n. 1, 2017, pp. 43–54.
- [3] Upadhye, H.R. and Kandlikar, S.G., Optimization of microchannel geometry for direct chip cooling using single phase heat transfer», *ASME 2nd Int. Conf. Microchannels and Minichannels*, Rochester, New York, USA, Jan. 2004, pp. 679–685.
- [4] Wang, H., Chen, Z. and Gao, J., Influence of geometric parameters on flow and heat transfer performance of micro-channel heat sinks, *Appl. Therm. Eng.*, vol. 107, Aug. 2016, pp. 870–879.
- [5] Xie, X.L., Liu, Z.J., He, Y.L. and Tao, W.Q. Numerical study of laminar heat transfer and pressure drop characteristics in a water-cooled minichannel heat sink, *Appl. Therm. Eng.*, vol. 29, n. 1, 1009, pp. 64–74.
- [6] Hetsroni, G., Mosyak, A., Segal, Z. and Ziskind, G., A uniform temperature heat sink for cooling of electronic devices, *Int. J. Heat Mass Transf.*, vol. 45, n. 16, 2002, pp. 3275–3286.
- [7] T. N. Tran, M. W. Wambsganss, e D. M. France, «Small circular-and rectangular-channel boiling with two refrigerants», *Int. J. Multiph. Flow*, vol. 22, n. 3, pp. 485–498, 1996.
- [8] Teodori, E., Pontes, P., Moita and A.S., Moreira, A.L.N., Thermographic analysis of interfacial heat transfer mechanisms on droplet/wall interactions with high temporal and spatial resolution, *Exp. Thermal Fluid Sci.*, vol. 96, 2018, pp. 284-294.
- [9] Georgoulas, A., Koukouvini, P., Gavaises, M. and Marengo, M., Numerical investigation of quasi-static bubble growth and detachment from submerged orifices in isothermal liquid pools: The effect of varying fluid properties and gravity levels, *Int. J. Multiph. Flow*. 74 2015, pp. 59–78.
- [10] Georgoulas, A., Andredaki, M. and Marengo, M., An enhanced VOF method coupled with heat transfer and phase change to characterize bubble detachment in saturated pool boiling, *Energies*, vol., 10, 2017.
- [11] Vontas, K., Andredaki, M., Georgoulas, A., Miché, N. and Marengo M., The effect of surface wettability on flow boiling characteristics within microchannels, *Int. J. Heat Mass Transf.* vol.172, 2021, 121133.